AGU PUBLICATIONS

Geophysical Research Letters

RESEARCH LETTER
10.1002/2015GL066811

**Key Points:**
- Amphibian electrical resistivity section from a passive continental margin
- Walvis ridge offshore associated with thickened crust with moderate electrical resistivity
- Electrically conductive Proterozoic Mobile Belt shear zones unaffected by continental break-up

**Supporting Information:**
- Text S1 and Figures S1–S9

**Correspondence to:**
O. Ritter,
oritter@gfz-potsdam.de

**Citation:**
Kapinos, G., U. Weckmann, M. Jegen-Kulcsar, N. Meqbel, A. Neska, T. T. Katjiuongua, S. Hoelz, and O. Ritter (2016), Electrical resistivity image of the South Atlantic continental margin derived from onshore and offshore magnetotelluric data, *Geophys. Res. Lett.*, *43*, 154–160, doi:10.1002/2015GL066811.

Received 29 OCT 2015
Accepted 13 DEC 2015
Accepted article online 16 DEC 2015
Published online 14 JAN 2016



# Electrical resistivity image of the South Atlantic continental margin derived from onshore and offshore magnetotelluric data

**G. Kapinos[1,2], U. Weckmann[1], M. Jegen-Kulcsar[3], N. Meqbel[1], A. Neska[4], T. T. Katjiuongua[5], S. Hoelz[3], and O. Ritter[1,6]**

[1]GFZ German Research Centre for Geosciences, Potsdam, Germany, [2]Now at Federal Institute for Geosciences and Natural Resources (BGR), Hannover, Germany, [3]GEOMAR Helmholtz Centre for Ocean Research Kiel, Kiel, Germany, [4]Institute of Geophysics, Polish Academy of Sciences, Warszawa, Poland, [5]Geological Survey of Namibia, Ministry of Mines and Energy, Windhoek, Namibia, [6]Freie Universität Berlin, Institute of Geophysics, Berlin, Germany

**Abstract** We present a deep electrical resistivity image from the passive continental margin in Namibia. The approximately 700 km long magnetotelluric profile follows the Walvis Ridge offshore, continues onshore across the Kaoko Mobile Belt and reaches onto the Congo Craton. Two-dimensional inversion reveals moderately resistive material offshore, atypically low for oceanic lithosphere, reaching depths of 15–20 km. Such moderate resistivities are consistent with seismic *P* wave velocity models, which suggest up to 35 km thick crust. The Neoproterozoic rocks of the Kaoko Mobile Belt are resistive, but NNW-striking major shear-zones are imaged as subvertical, conductive structures in the upper and middle crust. Since the geophysical imprint of the shear zones is intact, opening of the South Atlantic in the Cretaceous did not alter the middle crust. The transition into the cratonic region coincides with a deepening of the high-resistive material to depths of more than 60 km.

## 1. Introduction

The breakup of Western Gondwana and the opening of the South Atlantic in the early Cretaceous were accompanied by strong volcanic eruptions and the formation of the Parana-Etendeka flood basalts. The rifting process and the associated magmatic events can be traced offshore along the Walvis Ridge and the Rio Grande Rise. These two volcanic seamount chains, which today trace back to magmatic provinces on both sides of the Atlantic in Brazil and Namibia, are generally believed to mark plate motion over a hotspot (or thermal anomaly) during the last 130 Ma [e.g. *O'Connor and Duncan*, 1990; *Gladczenko et al.*, 1998]. It is still debated, however, if the triggering and controlling factors for the continental breakup were dominated by preexisting and reactivated structures (lithospheric weak zones) or by a huge (>1000 km in diameter) mantle plume and associated magmatism [e.g. *Buiter and Torsvik*, 2014; *Salomon et al.*, 2014; *VanDecar et al.*, 1995; *Storey*, 1995]. To tackle this fundamental geodynamic question, the South Atlantic with its conjugate continental margins in Namibia and Brazil was focus of a number of geophysical and geological investigations within a Special Priority Program of the German Science Foundation (DFG).

Previous magnetotelluric studies at the western South African margin are limited to (onshore) investigations of the Damara Belt [*Ritter et al.*, 2003; *Weckmann et al.*, 2003] and on the Archean Congo craton, east of our study area [*Weckmann*, 2012 and references therein; *Khoza et al.*, 2013; *Miensopust et al.*, 2011].

Figure 1 shows a map of the study area with onshore and offshore MT site locations. The Walvis Ridge forms an approximately 3400 km long volcanic seamount chain, trending NE-SW, from Africa to the mid-Atlantic Ridge. The broad eastern plateau of the Walvis Ridge, relevant for this study, extends seaward from the African coast to about 5°E. It was formed by large volumes of hot material which erupted along the plate boundary during the opening of the Atlantic [*O'Connor and Duncan*, 1990; *Duncan*, 1984]. While the Walvis Ridge has been evolving since the early Cretaceous, the evolution of the Kaoko Mobile Belt began in the Neoproterozoic and is related to the amalgamation of West Gondwana.

The Kaoko Belt formed by continental collision and oblique convergence of the Congo and the Rio de la Plata cratons and the closure of the northern Adamastor Ocean at 580–550 Ma. It has been described as a classic transpressional strike slip orogen with NNW striking sinistral shear zones, folds, and thrusts

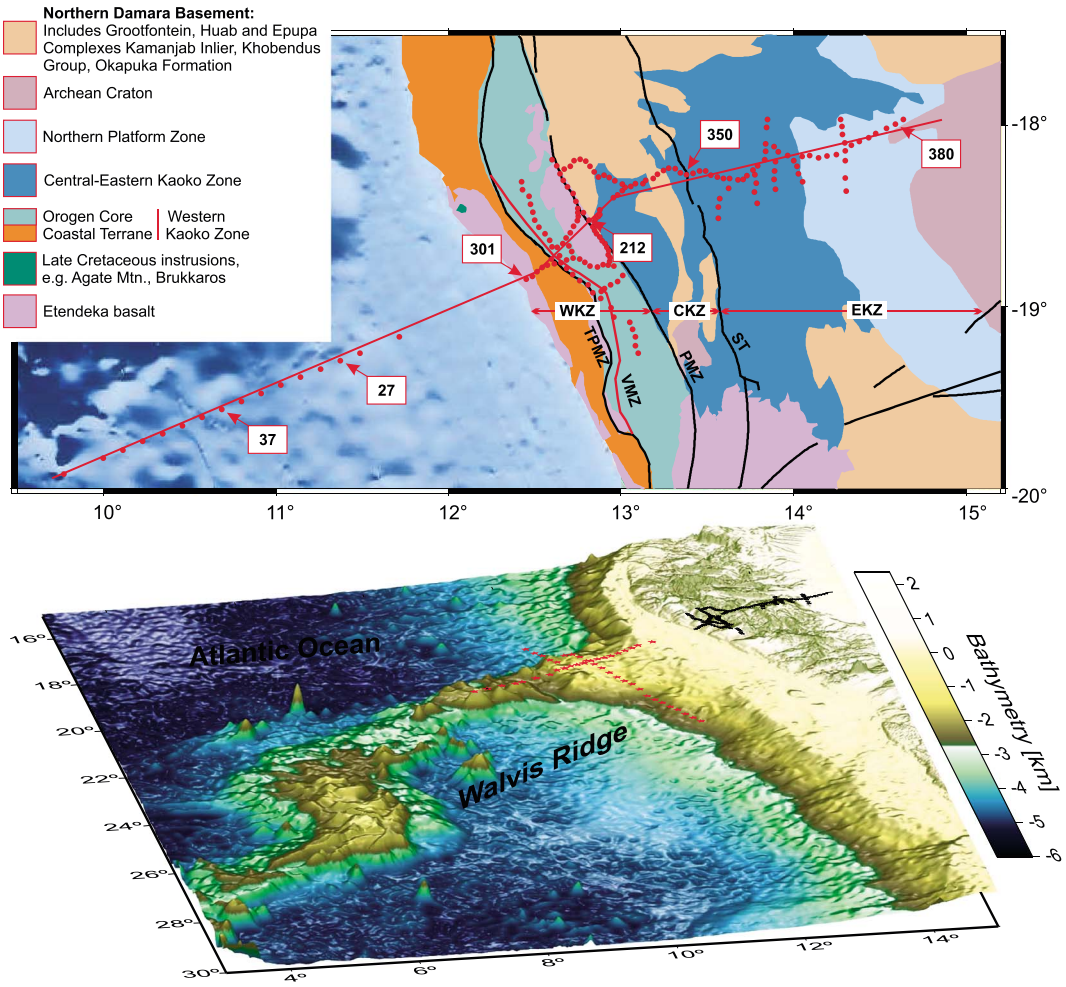


**Figure 1.** (top) Surface geological map of the Kaoko Belt showing lithotectonic units and major shear zones (bold lines), modified after *Goscombe et al.* [2003] and B. Corner (personal communication, 2010). WKZ: Western Kaoko Zone; CKZ: Central Kaoko Zone; EKZ: Eastern Kaoko Zone. Neoproterozoic shear zones: TPMZ: Three Palms Mylonite Zone, VMZ: Village Mylonite Zone, PMZ: Purros Mylonite Zone, ST: Sesfontein Thrust. Red dots indicate MT stations, the red line shows the location of the onshore-offshore profile. Numbers in boxes indicate names of some selected MT stations. (bottom) Colors indicate bathymetry of the Walvis Ridge.

[*Goscombe et al.*, 2003]. The rocks of the Kaoko Belt comprise of a mosaic of Archean, Paleoproterozoic, and Mesoproterozoic basement with igneous rocks and low-to-high grade metamorphic signature [*Goscombe et al.*, 2003; *Foster et al.*, 2009].

The Kaoko Belt can be subdivided into three NNW-trending zones with distinct tectonic and metamorphic properties [*Miller*, 1983]—the Western (WKZ), Central (CKZ), and Eastern (EKZ) Kaoko zones (see Figure 1). In the WKZ the poorly exposed Three Palm Mylonite Zone (TPMZ) separates the Orogen Core from the Coastal Terrane. The latter has been described as an exotic tectonostratigraphic outboard arc terrane which docked to the former continental margin of the Congo Craton by oblique collision and crustal overriding [*Goscombe and Gray*, 2007; *Foster et al.*, 2009; *Frimmel et al.*, 2011]. East of the TPMZ, granites and basement slivers of different metamorphic grades are exposed [*Foster et al.*, 2009; *Goscombe et al.*, 2003]. The eastern border of the WKZ is marked by the Purros Mylonite Zone (PMZ); a network of interlinked crustal ductile shear zones, which can be traced for at least 500 km, and is characterized by a lateral displacement of $>$50 km resulting in high shear strains and ductile deformation, mylonitic or ultramylonitic fabric/foliation, and steep dip [*Goscombe et al.*, 2003]. The eastern margin of the Central Kaoko Zone and the transition to the Foreland is marked by the Sesfontein Thrust (ST), a major structural discontinuity in the Kaoko Belt which was formed under brittle-ductile conditions in the late stage of Damara Orogeny [*Goscombe et al.*, 2003;

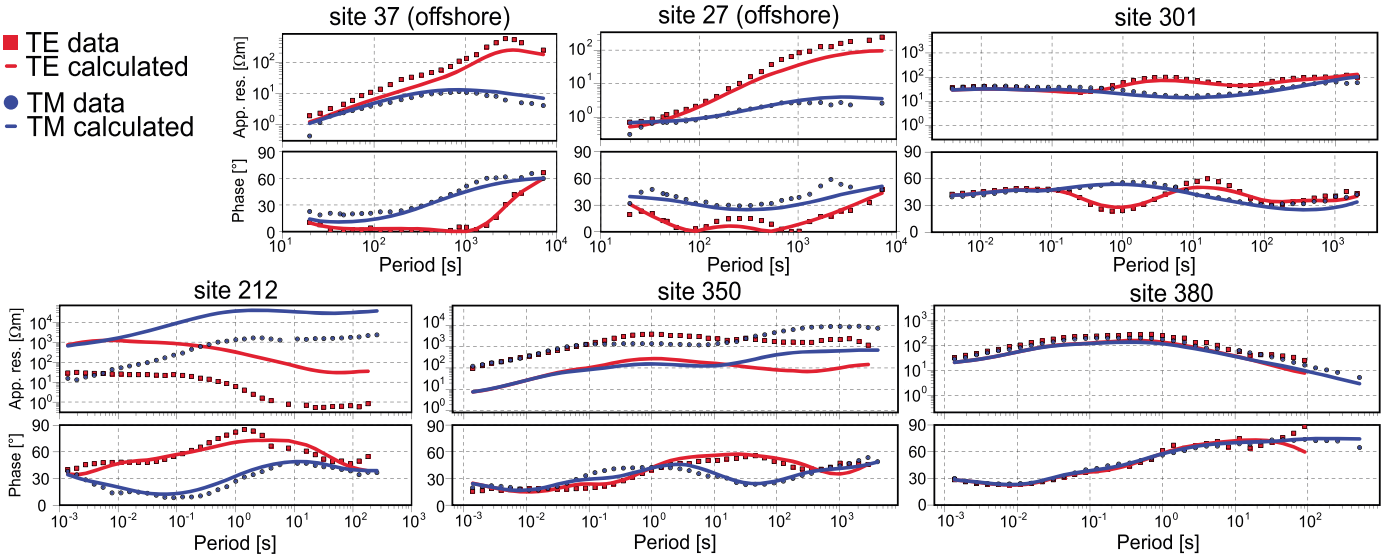


**Figure 2.** Exemplary apparent resistivity and phase curves: Stations 37 and 27 are located offshore on the Walvis Ridge. Stations 301, 212, 350, and 380 are representative for the onshore data (Kaoko Belt and Congo Craton); see Figure 1 for more details. The solid lines are 2-D inversion responses (see text).

*Frimmel et al.*, 2011]. The thrust separates high-grade metamorphic rocks in the west from very low grade metamorphic rocks further east [*Stanistreet and Charlesworth*, 2001].

The EKZ has been described as a Neoproterozoic molasse foreland overlying cratonic basement at the western margin of the Congo Craton [*Goscombe et al.*, 2003; *Frimmel et al.*, 2011].

## 2. Magnetotelluric Data

The magnetotelluric onshore data were acquired in October and November 2011 at 167 sites in an approximately 140 km wide and 260 km long corridor. Site spacing varied between 2 and 5 km, which ensured good resolution for the anticipated highly complex structures of the Kaoko Belt. At each station five-component broadband MT data (10 kHz–1 mHz) were recorded, typically for 3 days. We used the robust remote-reference processing algorithm described in *Ritter et al.* [1998] and *Weckmann et al.* [2005] to process the onshore data.

Ocean bottom MT data (OBMT) data were collected between 320 m and 4150 m water depth at 45 sites along two profiles, parallel and perpendicular to the Walvis Ridge (here we consider only the data along the Walvis Ridge). The spacing between OBMT sites varied between 12 and 30 km. Data were recorded for approximately 3 weeks with a sampling rate of 1 s, resulting in offshore MT data in a frequency range from 0.1 Hz–0.1 mHz which is different from those of the onshore data. To process the offshore data, we use the bounded influence algorithm of *Chave and Thomson* [2004] and the multistation scheme of *Egbert* [1997].

The obtained impedance tensor and vertical magnetic transfer function data (see Figure 2 and the supporting information) are generally of high quality, particularly in the remote areas of the WKZ (see Figure 1). However, large diagonal components of impedance tensor, phases over 90° at some sites as well as a strong variability of transfer functions within short distances are indicative for an influence of 3-D structures. Three-dimensional inversion of the entire data set is not feasible, however, as the onshore and offshore data sets are too disparate with respect to site spacing and areal distribution. But 2-D inversion should only be attempted if subsets of the data can be identified which are consistent with 2-D assumptions.

We analyzed the impedance tensor data using the method given in *Becken and Burkhardt* [2004] and obtained a predominant north-south oriented regional strike direction (Figure 3 and the supporting information) for the sites along the profile marked in red in Figure 1. This strike direction is consistent with the orientation of the induction vectors (see Figures 3 and Figure S1 in the supporting information) and corresponds well with the expected regional trend of the tectonic structures of the Kaoko Belt. Thus, a 2-D interpretation of the data is justified but should be treated with caution, as not all of the complexity of the Kaoko Belt is accounted for. For the 2-D inversion, we assigned TE mode to the *Zxy* component

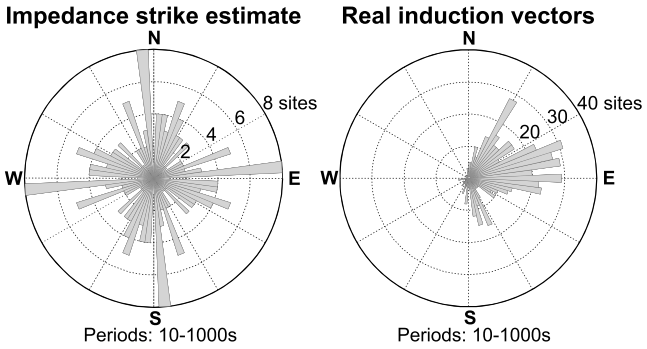


**Figure 3.** Geoelectric strike analysis: (left) impedances strike estimates after *Becken and Burkhardt* [2004] and (right) orientation of real induction vectors (Wiese convention) of stations along the profile (see Figure 1). The data indicate a NNW-SSE trending regional strike direction (inherent 90° ambiguity was addressed by consulting induction vectors).

of the impedance tensor, and we removed those parts of the data which were clearly inconsistent with 2-D assumptions (e.g., phases out of quadrant).

For the 2-D inversion, we used the nonlinear conjugate gradient inversion algorithm of *Rodi and Mackie* [2001] implemented in the WinGLink software package (Geosystem srl). After extensive testing, we eventually used a two-tier strategy which could cope with the strongly differing sensitivities of the onshore and offshore data (see supporting information, 2-D inversion of the data).

As a first step we inverted only the TM mode onshore data together with the vertical magnetic transfer functions. The TE-mode data were not considered at the beginning of the inversion procedure, as they are more strongly affected by the 3-D ocean topography. The starting model included the Atlantic Ocean (0.3 Ωm) and a crude bathymetry of the Walvis Ridge containing a 1–3 km thick layer of seafloor sediments on top with a conductivity gradient of 1 to 8 Ωm. All other regions of the starting model were set to 100 Ωm.

In a second step, we used the outcome of the initial inversion as input (starting model) for a joint inversion of the onshore and offshore data but now including all components (TE, TM, and induction vectors; see supporting information). The result of this 2-D inversion approach is shown in Figure 4.

The bathymetry plays a far more important role in marine MT than topography in onshore data. To assess the robustness of the 2-D inversion results with respect to bathymetry, we performed 3-D forward modeling using ModEM [*Egbert and Kelbert*, 2012; *Meqbel*, 2009] to estimate the coast effect and the effect of the

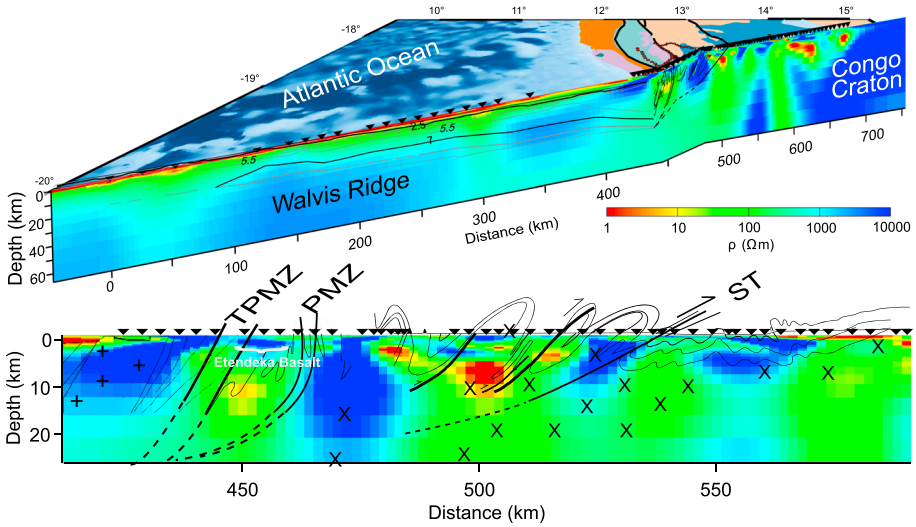


**Figure 4.** Two-dimensional inversion result following the profile line in Figure 1. Overall Red and yellow colors indicate regions of low electrical resistivity. Contour lines on the offshore section are taken from a *P* wave velocity models along the same profile [*Fromm et al.*, 2015]. Superimposed for comparison are the bathymetry of the Atlantic Ocean and major lithotectonic units of the study area (onshore); see Figure 1 for further details. The bottom part shows a close-up of the Kaoko-Belt subsection, overlain by tectonic structures taken from *Goscombe et al.* [2003]. Thick lines indicate major ductile shear zones: TPMZ: Three Palms Mylonite Zone, PMZ: Purros Mylonite Zone, and ST: Sesfontein Thrust. Thinner lines indicate syn deduced and antiforms deduced from geological mapping, crosses mark areas of inferred Mesoproterozoic and Paleoproterozoic basement gneisses.

bathymetry which is substantial along the offshore profile. The 3-D mesh design is a compromise between properly discretizing the complex bathymetry of the Walvis Ridge (Figure 1) and available computational resources. We ended up with an equidistant grid with cell sizes of 5 km × 5 km in the model core and increasing cell widths toward the periphery, in accordance with the exponential decay of the EM fields (see Figure S7). In the vertical direction we used generally uniform layer thicknesses of 100 m, but we refined the grid cells at the ocean bottom to ~20 m close to site locations. We also set the resistivity of the uppermost vertical cells (contact to the ocean water) above the sites to 1 Ωm to minimize numerical issues.

The responses (apparent resistivities and phases) of a simple 3-D model consisting only of a homogeneous half space (1000 Ωm) and the ocean (0.3 Ωm) clearly show the effect of the bathymetry (and a strong period dependency) but they do not resemble the offshore data (see supporting information). As a next step, we added a layer of higher conductivity (1 Ωm) close to the seafloor, in accordance with the observed sedimentary cover. Now the general shape of the apparent resistivity and phase curves is much more similar to the measured and modeled offshore data. In fact, the model appears as a simplified image of the resistivity structure obtained from 2-D inversion (offshore part, Figure 4). Since the calculated transfer functions of the simple 3-D model can reproduce the trend of the data and the 2-D inversion results, we conclude that the bathymetry can be described in 2-D, i.e., off-profile bathymetry appears to affect the data collected along the profile less as originally suspected.

## 3. Discussion

The 2-D inversion model in Figure 4 retained the 1–3 km thick conductive layer on top of the Walvis Ridge. This layer represents seafloor sediments which vary in thickness between several hundred meters in the western part to about 3 km in the east (H. Schulz, personnal communication, 2013). Down to depths of approximately 20 km, we observe for the offshore part of the section increasing resistivities of 30–300 Ωm (corresponding to a transition from green to blue colors in Figure 4). When compared with other marine studies [*Constable and Cox*, 1996; *Key*, 2012; *Heinson and Constable*, 1992], however, we observe a much thicker zone of moderately resistive material in the range of a few tens to a few hundred Ωm. Typical resistivity values for oceanic lithosphere are often found to exceed 1000 Ωm. Such high resistivities are reached in our section but only beyond depths of approximately 20 km. The observed moderate resistivities are more in line with continental crust than typical thin oceanic crust. This result is supported by recent seismic data. Based on *P* wave velocity models along the same profile, *Fromm et al*. [2015] suggest that the Walvis Ridge consists of closely spaced seamounts with up to 35 km thick crust. While crustal velocities of 5.5–7.2 km/s point to a gabbroic composition, the oceanic crust seems to be thickened (see also Figure 4).

Unfortunately, there is a substantial gap of almost 100 km between the onshore and offshore MT station layout which prevents a more detailed interpretation of the transition onto the continental shelf.

The westernmost part of the onshore profile crosses the Etendeka flood basalt region and the system of prominent NNW striking shear zones. According to *Milner et al*. [1992] and *Salomon et al*. [2014], the Etendeka formation does not reach deeper than approximately 880 m in the main outcrop area which is further south of the MT profile. In the resistivity section, the Etendeka basalts appear as a very resistive, subhorizontal flat and about 1 km thick layer, which is covered in the Khumib river valley with more conductive material. In contrast, the prominent shear zones, such as the PMZ, VMZ, and TPMZ (see Figure 1), are associated with very low resistivity (red colors in Figure 4). While it is difficult to associate individual fault strands with particular zones of high conductivity, it is clear that the high conductivity reaches to midcrustal depths (approximately 15 km). Fossil shear zones are often associated with high electrical conductivity because they can act as pathways for fluids, leading to ore mineralization or graphite enrichment, which in turn can have a lubricating effect and favor reactivation of the fault system [e.g., *Boerner et al*., 1996; *Wannamaker et al*., 2002; *Weckmann et al*., 2003; *Ritter et al*., 2005]. Mylonite shear zones typically contain minerals with larger grain boundaries than less-deformed, fine-grained regions. A geometrical model of less-conducting cubic grains and more-conducting grain boundaries, developed by *ten Grotenhuis et al*. [2004], predicts 1.5–2 orders of magnitude lower resistivity for the large grain sizes. The shear zones in the Kaoko Belt are of Neoproterozoic age, much older than the Cretaceous flood basalt events. Considering a voluminous emplacement of the flood basalts we either expect these faults to have served as pathways or

to have experienced thermal alteration. With laboratory measurements, *Yoshino and Noritake* [2011] show that the electrical conductivity decreases during annealing at high temperatures, possibly due to disconnection of the graphite or mineralized films and networks. Therefore, we conclude that the opening of the South Atlantic did not affect or considerably rework the middle crust of the Kaoko Belt. It would be highly unlikely though that any preexisting high conductivity could be preserved if the magmatic and thermal events had altered the deeper crust of the Kaoko Belt.

The lower crust and lithosphere of the Central Kaoko Zone (CKZ) seems to be dominated by moderate resistivities (around 100 Ωm), while the lithosphere of the EKZ appears to be predominantly resistive. The eastern boundary of the CKZ is marked by the Sesfontein Thrust (ST; Figure 1), which appears in the resistivity image as shallow westward dipping.

The easternmost part of the model reveals a deep rooted block with resistivities exceeding 10,000 Ωm which reach beyond the profile and which seems to correlate with the Precambrian Congo Craton. The resistivity section suggests that the cratonic material underlies the EKZ in the middle to lower crust. The transition between both units is marked by a clear conductivity contrast. Existing models [e.g., *Gray et al*., 2008 and references therein] imply a west dipping décollement, into which steeply dipping mylonite zones merge [*Goscombe et al*., 2005]. Below such a décollement, a basement consisting of cratonic rocks is suggested, located at midcrustal depth below the EKZ and deepening toward the boundary between the WKZ and the CKZ. Our 2-D inversion is inconsistent with such a tectonic model as the high resistivities typical for cratonic rocks appear at middle to lower crustal depth in the region of the EKZ but not in the CKZ. The regions of very low resistivity found in the EKZ and the adjacent craton should be interpreted with care, however, as these zones are introduced mainly by the TE-mode, which is more susceptible to off-profile structures and which cannot be explained with 2-D inversion.

## 4. Summary and Conclusions

We present 2-D inversion results from an amphibious (onshore and offshore) magnetotelluric profile across the passive continental margin in Northern Namibia. When compared with other marine studies we observe a much thicker zone of moderately resistive material which is atypical for oceanic lithosphere with expected resistivities exceeding 1000 Ωm. The observed resistivities are consistent though with recent seismic data which suggest up to 35 km thick crust for the Walvis Ridge seamounts [*Fromm et al*., 2015]. The Etendeka basalts appear as a localized, very resistive layer in the upper crust. In contrast, the prominent shear zones of the Kaoko Belt are associated with zones of very low resistivity which reach to midcrustal depths (approximately 15 km). Since these Neoproterozoic shear zones appear as contiguous features of low electrical resistivity, we infer they are still intact and conclude that opening of the South Atlantic in the Cretaceous did not alter the middle crust of the Kaoko Belt. The resistivity section suggests furthermore that the cratonic material underlies the Eastern Kaoko Zone in the middle to lower crust.

These results are consistent with plate motion over a hotspot or thermal anomaly during the last 130 Ma with associated localized magmatism on the Namibian passive margin. The preexisting Neoproterozoic shear zones of the Kaoko Belt, which are lithospheric weak zones, were not modified by the Cenozoic magmatic events. This would, however, to be expected for mantle plume associated magmatism (>1000 km in diameter).

**Acknowledgments**
We would like to acknowledge tremendous work by the members of the field team: M. Baumann, F. Eckelmann, J. Guerreros, A. Grayver, R. Klose, S. Rettig, P. Sass, S. Schennen, G. Schmidt, M. Schüler, K. Tietze, and S. Windhi Niasari. We thank G. Muñoz for his help with processing the data. We express our sincere thanks to G. Schneider and K.H. Hoffmann from the GS Namibia for administrational and logistics support. We gratefully acknowledge Paul van der Ploeg and his team for organizing a great field camp. The MT instruments were supplied by the Geophysical Instrument Pool Potsdam. We acknowledge funding from the German Science Foundation (SPP 1375, grant Ri 1127/11-1) and the GFZ German Research Centre for Geosciences.

## References

Becken, M., and H. Burkhardt (2004), An ellipticity criterion in magnetotelluric tensor analysis, *Geophys. J. Int.*, *159*(1), 69–82.
Boerner, D. E., R. D. Kurtz, and J. A. Craven (1996), Electrical conductivity and Paleo-Proterozoic foredeeps, *J. Geophys. Res.*, *101*(B6), 13,775–13,791, doi:10.1029/96JB00171.
Buiter, S. J., and T. H. Torsvik (2014), A review of Wilson Cycle plate margins: A role for mantle plumes in continental break-up along sutures?, *Gondwana Res.*, *26*, 627–653, doi:10.1016/j.gr.2014.02.007.
Chave, A. D., and D. J. Thomson (2004), Bounded influence magnetotelluric response function estimation, *Geophys. J. Int.*, *157*(3), 988–1006.
Constable, S., and C. S. Cox (1996), Marine controlled-source electromagnetic sounding: 2. The PEGASUS experiment, *J. Geophys. Res.*, *101*(B3), 5519–5530, doi:10.1029/95JB03738.
Duncan, R. A. (1984), Age progressive volcanism in the New England seamounts and the opening of the central Atlantic Ocean, *J. Geophys. Res.*, *89*(B12), 9980–9990, doi:10.1029/JB089iB12p09980.
Egbert, G. D. (1997), Robust multiple-station magnetotelluric data processing, *Geophys. J. Int.*, *130*(2), 475–496.
Egbert, G. D., and A. Kelbert (2012), Computational recipes for electromagnetic inverse problems, *Geophys. J. Int.*, *189*(1), 251–267.

Foster, D. A., B. D. Goscombe, and D. R. Gray (2009), Rapid exhumation of deep crust in an obliquely convergent orogen: The Kaoko Belt of the Damara Orogen, *Tectonics*, *28*, TC4002, doi:10.1029/2008TC002317.

Frimmel, H. E., M. S. Basei, and C. Gaucher (2011), Neoproterozoic geodynamic evolution of SW-Gondwana: A southern African perspective, *Int. J. Earth Sci. (Geol Rundsch)*, *100*, 323–354.

Fromm, T., L. Planert, W. Jokat, T. Ryberg, J. H. Behrmann, M. H. Weber, and C. Haberland (2015), South Atlantic opening: A plume-induced breakup?, *Geology*, *43*, 931–934, doi:10.1130/G36936.1.

Gladczenko, T. P., J. Skogseid, and O. Eldhom (1998), Namibia volcanic margin, *Mar. Geophys. Res.*, *20*, 313–341.

Goscombe, B., M. Hand, and D. Gray (2003), Structure of the Kaoko Belt, Namibia: Progressive evolution of a classic transpressional orogen, *J. Struct. Geol.*, *25*(7), 1049–1081.

Goscombe, B., D. R. Gray, and M. Hand (2005), Extrusional tectonics in the core of a transpressional orogen: The Kaoko Belt, Namibia, *J. Petrol.*, *46*, 1203–1241.

Goscombe, B. D., and D. Gray (2007), The Coastal Terrane of the Kaoko Belt, Namibia: Outboard arc-terrane and tectonic significance, *Precambrian Res.*, *155*, 139–158.

Gray, D. R., D. A. Foster, J. G. Meert, B. D. Goscombe, R. Armstrong, R. A. J. Trouw, and C. W. Passchier (2008), A Damara orogen perspective on the assembly of southwestern Gondwana, *Geol. Soc. London, Spec. Publ.*, *294*, 257–278.

Heinson, G., and S. Constable (1992), The electrical conductivity of the oceanic upper mantle, *Geophys. J. Int.*, *110*(1), 159–179.

Key, K. (2012), Marine electromagnetic studies of seafloor resources and tectonics, *Surv. Geophys.*, *33*(1), 135–167.

Khoza, T. D., A. G. Jones, M. R. Muller, R. L. Evans, M. P. Miensopust, and S. J. Webb (2013), Lithospheric structure of an Archean craton and adjacent mobile belt revealed from 2-D and 3-D inversion of magnetotelluric data: Example from southern Congo craton in northern Namibia, *J. Geophys. Res. Solid Earth*, *118*, 4378–4397, doi:10.1002/jgrb.50258.

Meqbel, N. M. M. (2009), The electrical conductivity structure of the Dead Sea Basin derived from 2D and 3D inversion of magnetotelluric data, doctoral dissertation, Freie Univ. Berlin, Germany.

Miensopust, M. P., A. G. Jones, M. R. Muller, X. Garcia, and R. L. Evans (2011), Lithospheric structures and Precambrian terrane boundaries in northeastern Botswana revealed through magnetotelluric profiling as part of the Southern African Magnetotelluric Experiment, *J. Geophys. Res.*, *116*, B02401, doi:10.1029/2010JB007740.

Miller, R. M. G. (1983), The Pan-African Damara Orogen of Namibia, in *The Damara Orogen*, *Spec. Publ. Geol. Soc. S. Afr.*, vol. 11, edited by R. M. G. Miller, pp. 431–515.

Milner, S. C., A. R. Duncan, and A. R. Ewart (1992), Quartz latite rheoignimbrite flows of the Etendeka Formation, north-western Namibia, *Bull. Volcanol.*, *54*, 200–219.

O'Connor, J., and R. Duncan (1990), Evolution of the Walvis Ridge–Rio Grande rise hot spot system: Implications for African and South American plate motions over plumes, *J. Geophys. Res.*, *95*(B11), 17,475–17,502, doi:10.1029/JB095iB11p17475.

Ritter, O., A. Junge, and G. Dawes (1998), New equipment and processing for magnetotelluric remote reference observations, *Geophys. J. Int.*, *132*, 535–548.

Ritter, O., U. Weckmann, T. Vietor, and V. Haak (2003), A magnetotelluric study of the Damara Belt in Namibia 1. Regional scale conductivity anomalies, *Phys. Earth Planet. Inter.*, *138*, 71–90, doi:10.1016/S0031-9201(03)00078-5.

Ritter, O., A. Hoffmann-Rothe, P. A. Bedrosian, U. Weckmann, and V. Haak (2005), Electrical conductivity images of active and fossil fault zones, in *High-Strain Zones: Structure and Physical Properties*, *Geol. Soc. London Spec. Publ.*, vol. 245, edited by D. Bruhn and L. Burlini, pp. 165–186.

Rodi, W., and R. L. Mackie (2001), Nonlinear conjugate gradients algorithm for 2-D magnetotelluric inversion, *Geophysics*, *66*(1), 174–187, doi:10.1190/1.1444893.

Salomon, E., D. Koehn, and C. Passchier (2014), Brittle reactivation of ductile shear zones in NW Namibia in relation to South Atlantic rifting, *Tectonics*, *34*, 70–85, doi:10.1002/2014TC003728.

Stanistreet, I. G., and E. G. Charlesworth (2001), Damaran basement-cored fold nappes incorporating pre-collisional basins, Kaoko Belt, Namibia, and controls on Mesozoic supercontinental break-up, *S. Afr. J. Geol.*, *104*, 1–12.

Storey, B. C. (1995), The role of mantle plumes in continental breakup: Case histories from Gondwanaland, *Nature*, *377*, 301–308, doi:10.1038/377301a0.

ten Grotenhuis, S. M., M. R. Drury, C. J. Peach, and C. J. Spiers (2004), Electrical properties of fine-grained olivine: Evidence for grain boundary transport, *J. Geophys. Res.*, *109*, B06203, doi:10.1029/2003JB002799.

VanDecar, J., D. James, and M. Assumpção (1995), Seismic evidence for a fossil mantle plume beneath South America and implications for plate driving forces, *Nature*, *378*, 25–31, doi:10.1038/378025a0.

Wannamaker, P. E., G. R. Jiracek, J. A. Stodt, G. T. Caldwell, V. M. Gonzalez, J. D. McKnight, and A. D. Porter (2002), Fluid generation and pathways beneath an active compressional orogen, the New Zealand Southern Alps, inferred from magnetotelluric data, *J. Geophys. Res.*, *107*(B6), 2117, doi:10.1029/2001JB000186.

Weckmann, U. (2012), Making and breaking of a continent—What can we learn from MT in Africa?, *Surv. Geophys.*, *33*, 107–134.

Weckmann, U., O. Ritter, and V. Haak (2003), A magnetotelluric study of the Damara Belt in Namibia 2. MT phases over 90° reveal the internal structure of the Waterberg Fault/Omaruru Lineament, *Phys. Earth Planet. Inter.*, *138*, 91–112.

Weckmann, U., A. Magunia, and O. Ritter (2005), Effective noise separation for magnetotelluric single site data processing using a frequency domain selection scheme, *Geophys. J. Int.*, *161*(3), 635–652.

Yoshino, T., and F. Noritake (2011), Unstable graphite films on grain boundaries in crustal rocks, *Earth Planet. Sci. Lett.*, *306*(3–4), 186–192, doi:10.1111/j.1365-246X.2005.02621.x.